

Novel pharmaceutical cocrystals of triflusal: crystal engineering and physicochemical characterization

Srinivasulu Aitipamula,^{*,a} Lucy K. Mapp,^{a,b} Annie B. H. Wong,^a Pui Shan Chow,^a and Reginald B.H. Tan^{*,a,c}

^a*Crystallization and Particle Science, Institute of Chemical and Engineering Sciences, A*STAR (Agency for Science, Technology and Research), 1, Pesek Road, Jurong Island, Singapore, 627833. Tel: (65) 6796 3858, Fax: (65) 6316 6183.*

Email: srinivasulu_aitipamula@ices.a-star.edu.sg

^b*Chemistry, Faculty of Natural and Environmental Sciences, University of Southampton, University Road, SO17 1BJ, United Kingdom.*

^c*Department of Chemical & Biomolecular Engineering, National University of Singapore, 4 Engineering Drive 4, Singapore 117576.*

Email: reginald_tan@ices.a-star.edu.sg

Electronic Supplementary Information

(20 Pages)

Contents

Table S1	Details of coformers and method of cocrystallization used for the cocrystal screening and the product of cocrystallization
Fig. S1	Crystal structure of HTB-NA cocrystal
Fig. S2	ORTEP plots of the crystal structures
Figs. S3-S8	Comparison of the PXRD patterns of the grinding samples
Fig. S9	TG/TDA profile of triflusal-INA cocrystal
Fig. S10	TG/TDA profile of triflusal-VA cocrystal
Fig. S11	Photomicrographs of triflusal-INA cocrystal from HSM experiment
Fig. S12	Photomicrographs of triflusal-VA cocrystal from HSM experiment
Figs. S13-S25	Pawley fit plots of the experimental powder patterns of stability samples with unit cell of the cocrystals from single crystal XRD

Table S1. Details of coformers and method of cocrystallization used for the cocrystal screening and the product of cocrystallization (All the materials were characterized by either powder or single crystal X-ray diffraction).

S. No.	Coformer	Product of cocrystallization		
		Solution crystallization		Solid-state grinding
		Alcoholic solutions (methanol and ethanol)	THF/1,4-Dioxane	
1	Nicotinamide	HTB-nicotinamide cocrystal	♣	♣
2	Isonicotinamide	HTB-isonicotinamide cocrystal	Triflusal-isonicotinamide cocrystal	Triflusal-isonicotinamide cocrystal
3	2-Picolinamide	*	Triflusal-2-picolinamide cocrystal	Triflusal-2-picolinamide cocrystal
4	Benzamide	*	Triflusal-benzamide cocrystal	Triflusal-benzamide cocrystal
5	Adipamide	*	♣	♣
6	Propionamide	*	Triflusal-propionamide cocrystal	♣
7	Pyrazinamide	*	♣	♣
8	Saccharin	*	♣	♣
9	Acesulfame	*	♣	♣
10	4,4'-Bipyridine	HTB-4,4'-Bipyridine cocrystal	♣	♣
11	Valpromide	*	Triflusal-valpromide cocrystal	Triflusal-valpromide cocrystal

12	Urea	*	Triflusal-urea cocrystal	Triflusal-urea cocrystal
13	Hydroxyurea	*	♣	♣
14	Melamine	HTB-melamine cocrystal	♣	♣
15	pyridoxine	*	♣	♣

'*' represents physical mixture of HTB and coformer. '♣' represents physical mixture of triflusal and coformer.

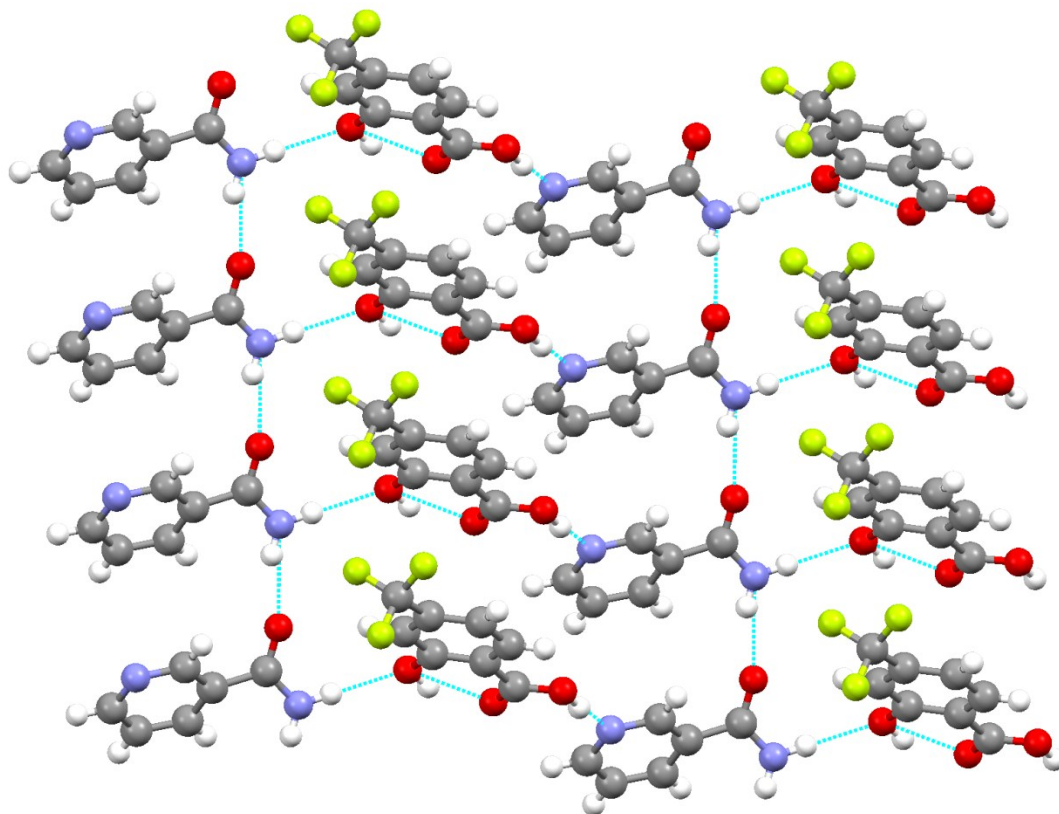


Fig. S1 Crystal structure of 1:1 HTB-NA cocrystal (Monoclinic, $P2_1/n$, $a = 5.0151 \text{ \AA}$, $b = 21.271 \text{ \AA}$, $c = 12.762 \text{ \AA}$, $\beta = 95.85^\circ$, $V = 1354.3 \text{ \AA}^3$).

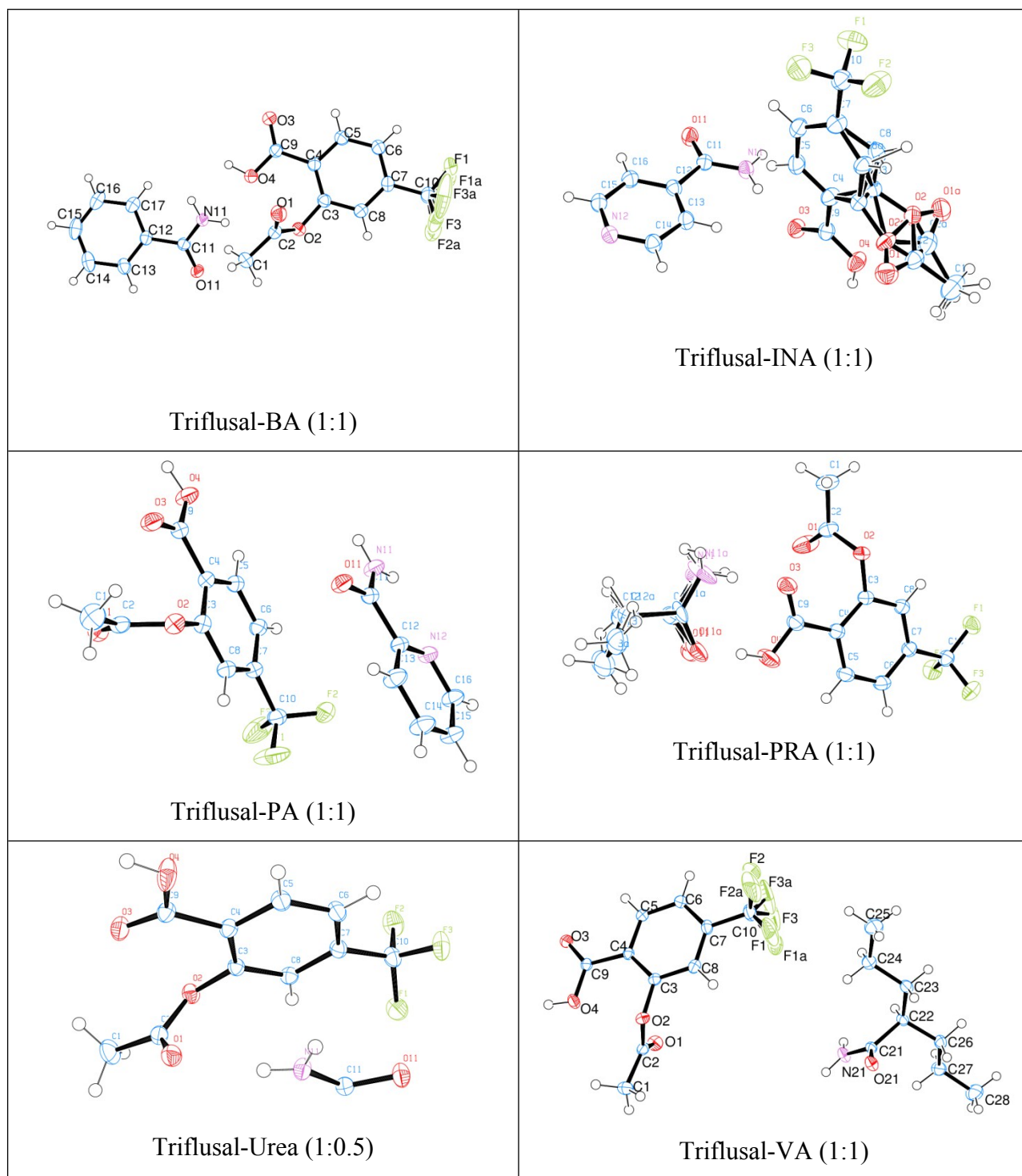


Fig. S2 ORTEP plots of the asymmetric units in the crystal structures of the triflusal cocrystals (thermal ellipsoids were drawn at 50 % probability).

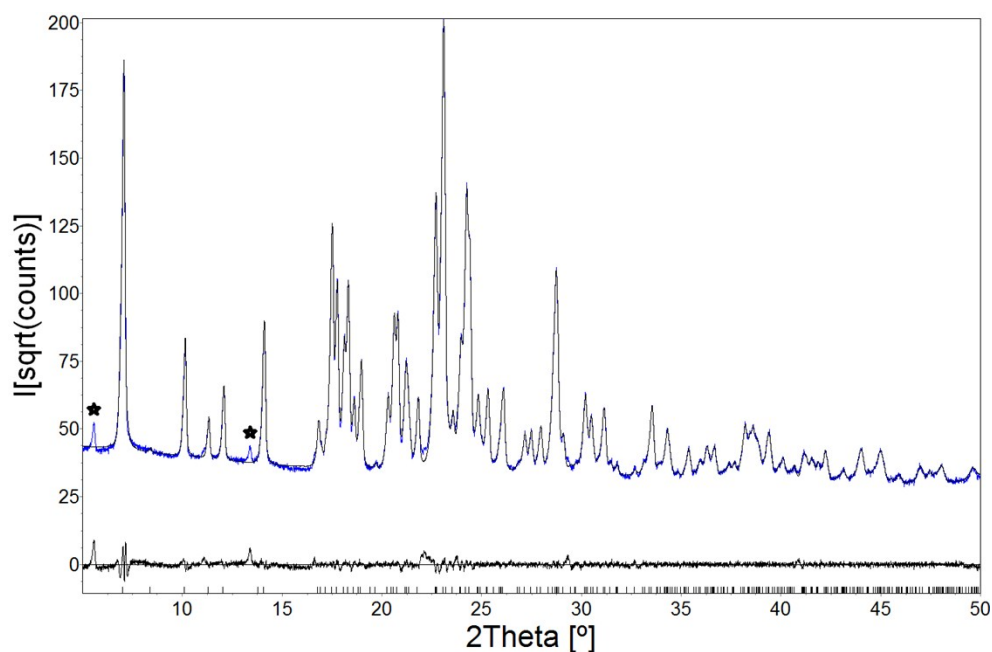
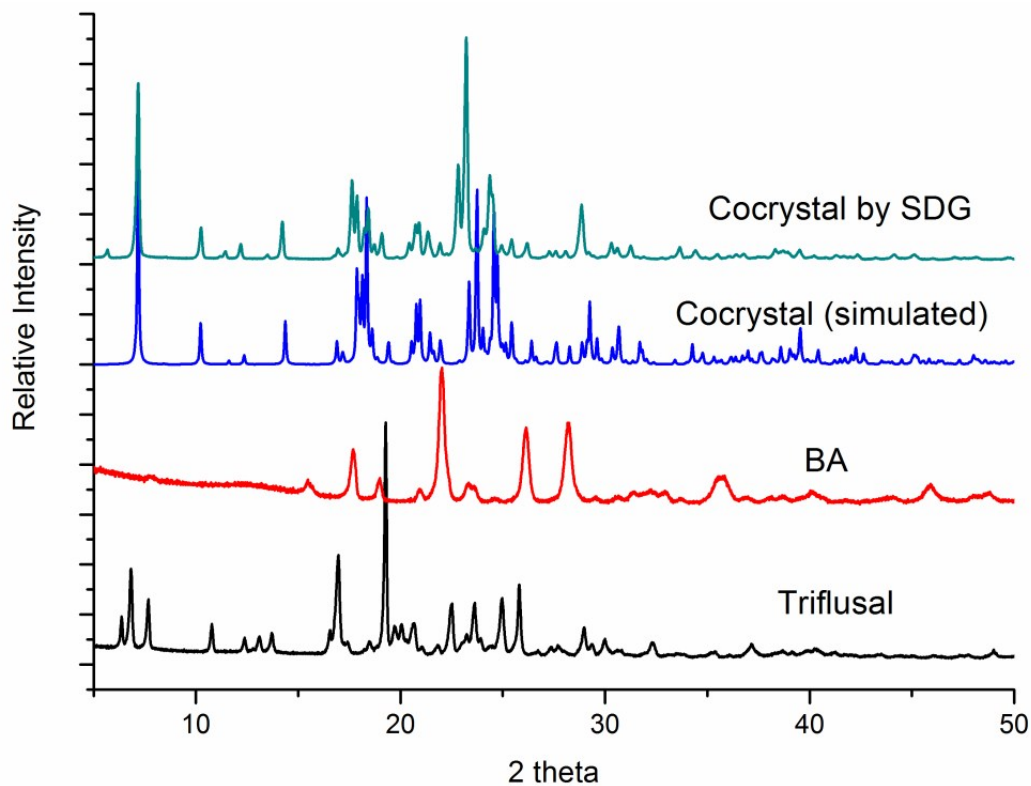


Fig. S3 Comparison of the PXRD patterns of the sample obtained in the solvent-drop grinding (SDG) experiment on 1:1 triflusal and BA with acetonitrile (top). Pawley fit of room temperature PXRD data with unit cell of triflusal-BA cocystal from single crystal XRD (bottom). The lattice parameters were refined freely. The peaks designated with star are unique and do not correspond to any of the starting materials and cocystal.

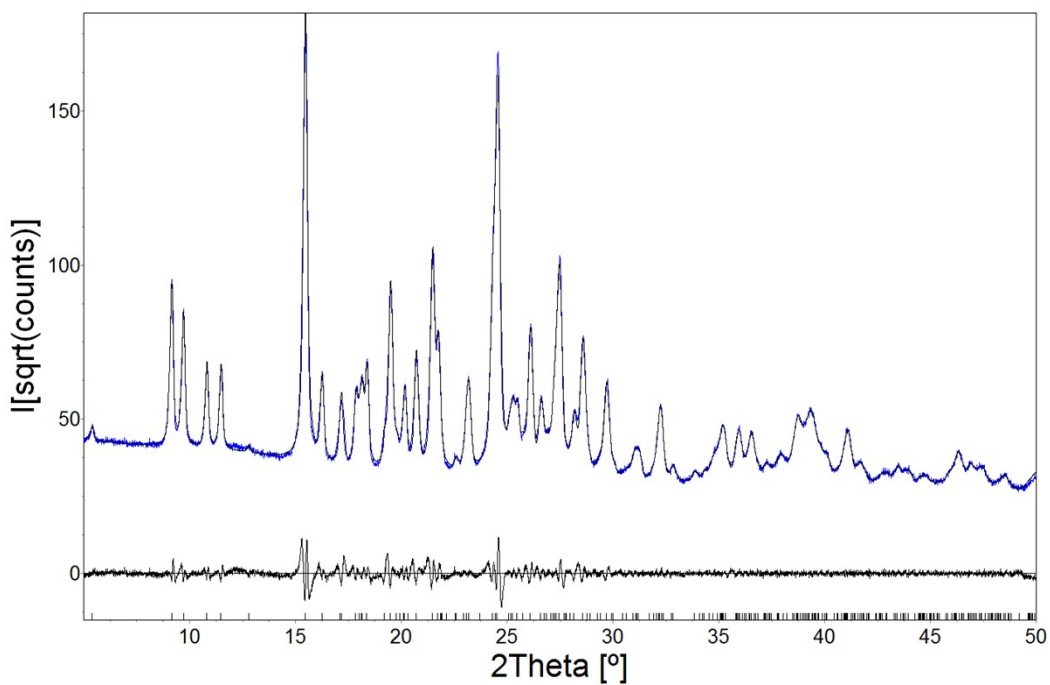
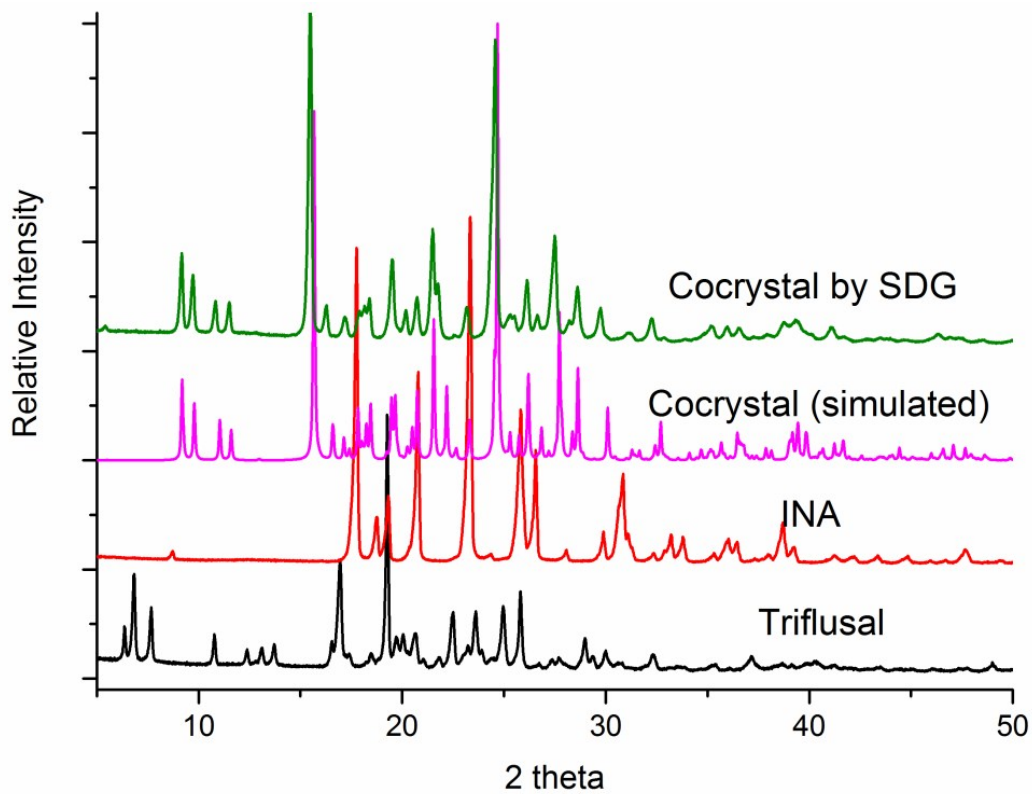


Fig. S4 Comparison of the PXRD patterns of the sample obtained in the SDG experiment on 1:1 triflusal and INA with acetonitrile (top). Pawley fit of room temperature PXRD data with unit cell of triflusal-INA cocrysal from single crystal XRD (bottom). The lattice parameters were refined freely.

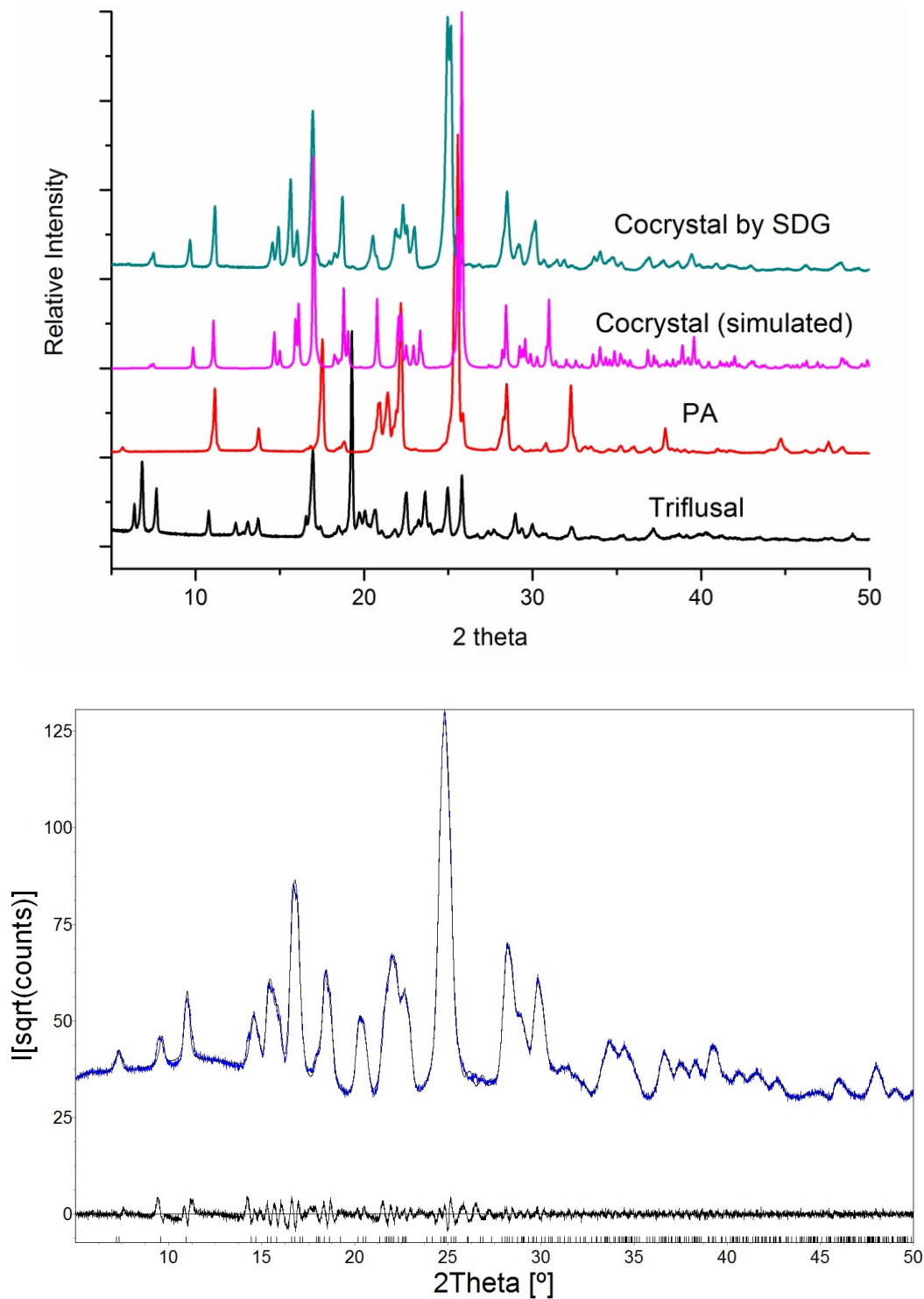


Fig. S5 Comparison of the PXRD patterns of the sample obtained in the SDG experiment on 1:1 triflusal and PA with acetonitrile (top). Pawley fit of room temperature PXRD data with unit cell of triflusal-PA cocrystal from single crystal XRD (bottom). The lattice parameters were refined freely.

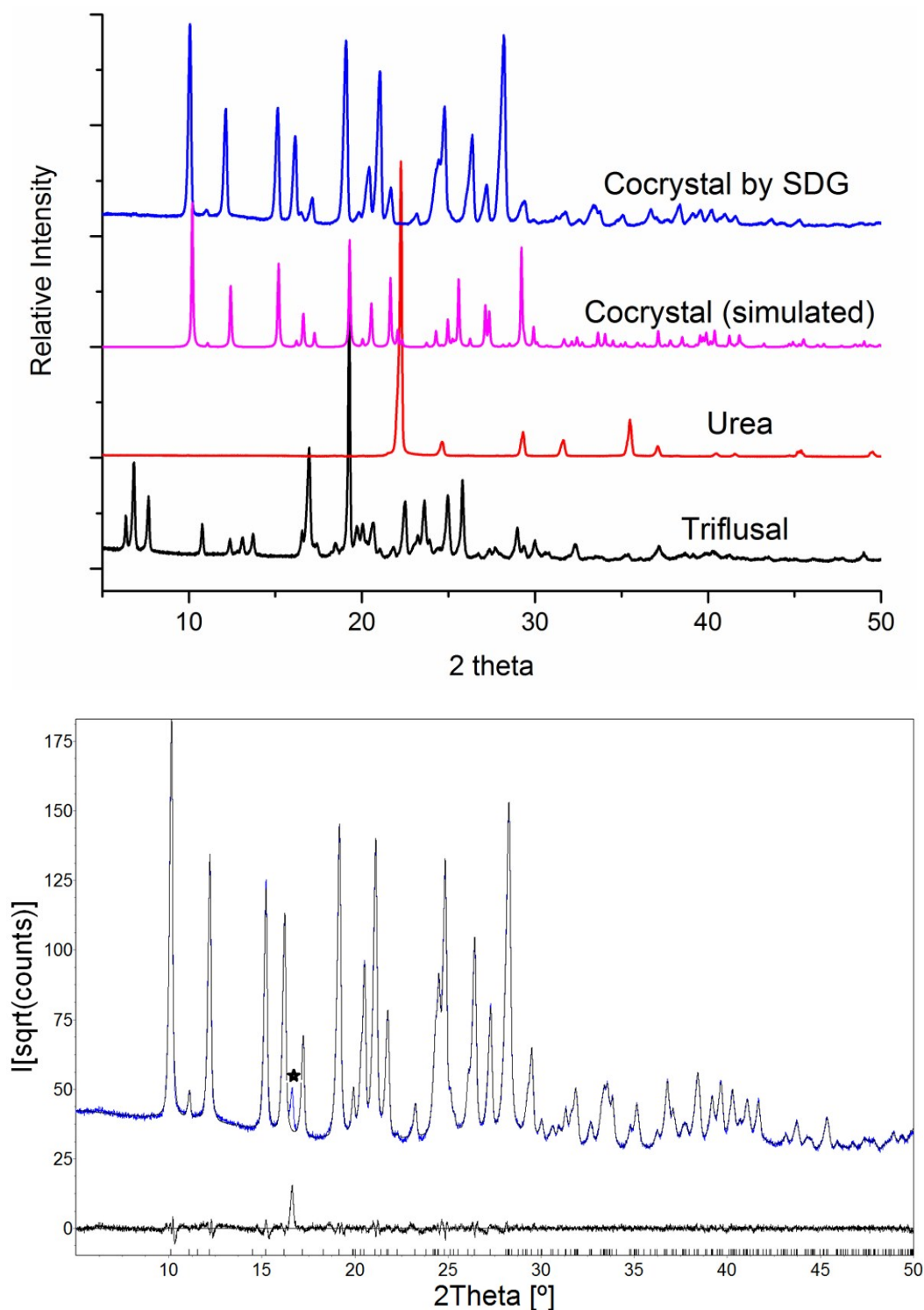


Fig. S6 Comparison of the PXR D patterns of the sample obtained in the SDG experiment on 1:0.5 triflusal and urea with acetonitrile (top). Pawley fit of room temperature PXR D data with unit cell of triflusal-urea cocrystal from single crystal XRD (bottom). The lattice parameters were refined freely. The peak designated with star is unique and do not correspond to any of the starting materials and cocrystal.

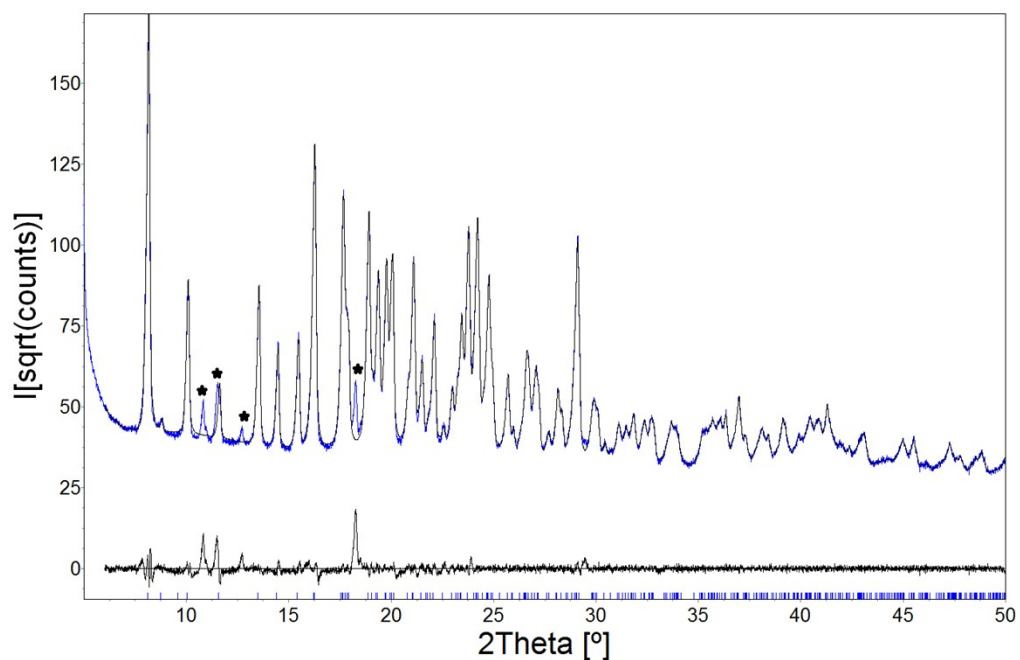
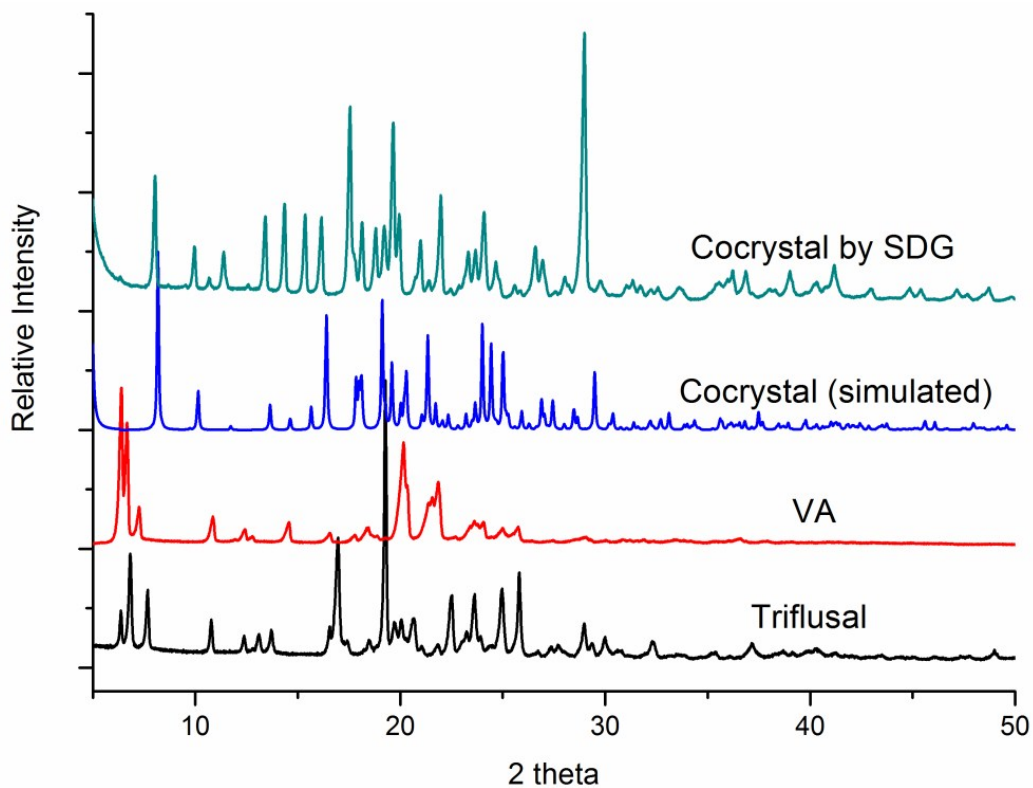


Fig. S7 Comparison of the PXRD patterns of the sample obtained in the SDG experiment on 1:1 triflusal and VA with acetonitrile (top). Pawley fit of room temperature PXRD data with unit cell of triflusal-VA cocrystal from single crystal XRD (bottom). The lattice parameters were refined freely. The peaks designated with star are unique and do not correspond to any of the starting materials and cocrystal.

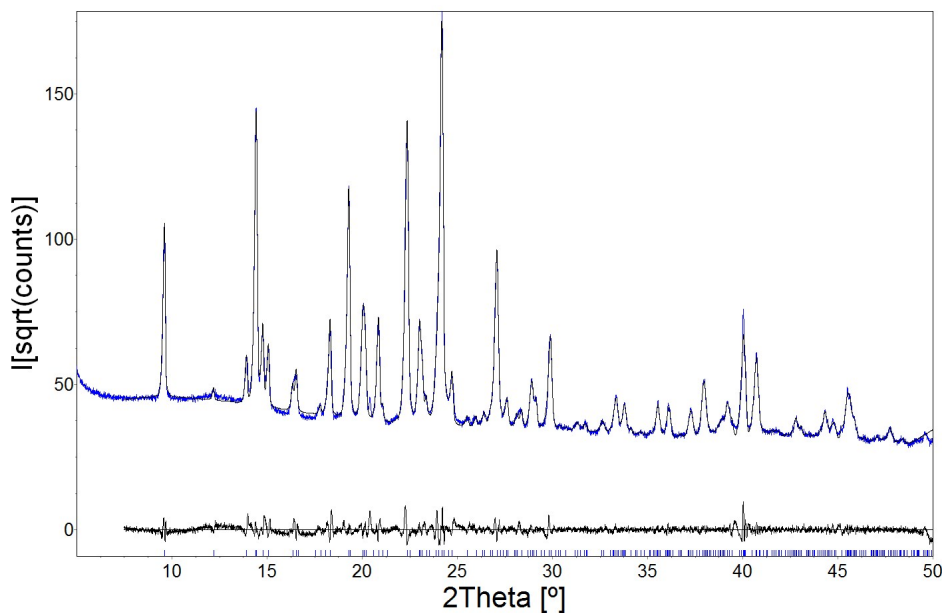
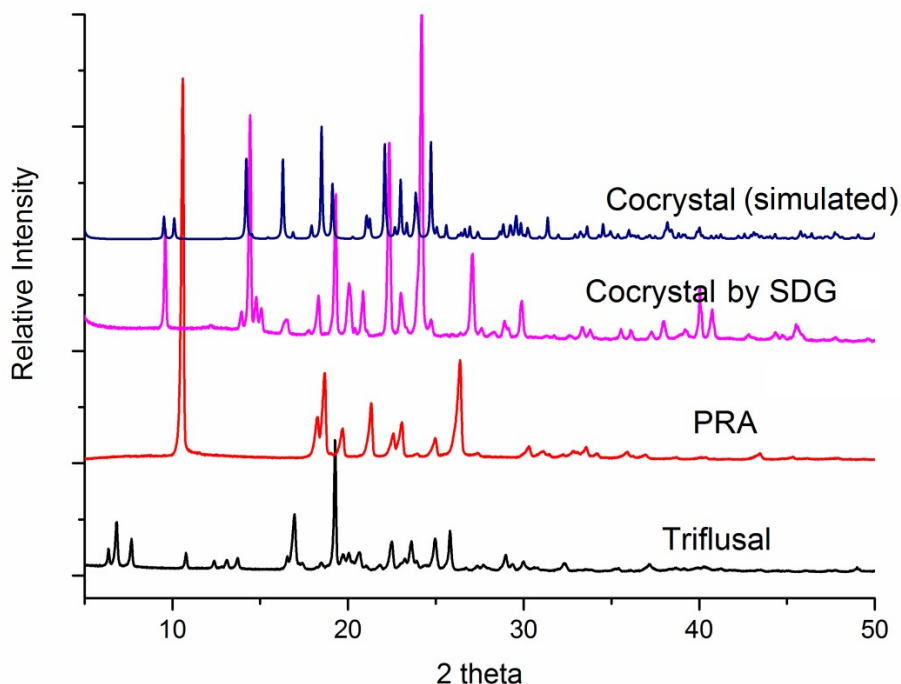


Fig. S8 Comparison of the PXRD patterns of the sample obtained in the SDG experiment on 1:1 triflusal and PRA with acetonitrile (top). Notice that the powder patterns do not match. Pawley fit of room temperature PXRD data with unit cell of triflusal-PRA cocrystal from single crystal XRD did not give a good match. Indexing the room temperature PXRD and subsequent Pawley fit (bottom) of the unit cell resulted in a different unit cell compared to the unit cell obtained from single crystal XRD 100 K due to lattice contraction. Unit cell from refinement: $a = 18.5120 \text{ \AA}$, $b = 7.8886 \text{ \AA}$, $c = 10.7903 \text{ \AA}$, $\beta = 97.20^\circ$; Unit cell from crystal structure (100 K): $a = 18.729 \text{ \AA}$, $b = 9.921 \text{ \AA}$, $c = 8.067 \text{ \AA}$, $\beta = 97.60^\circ$.

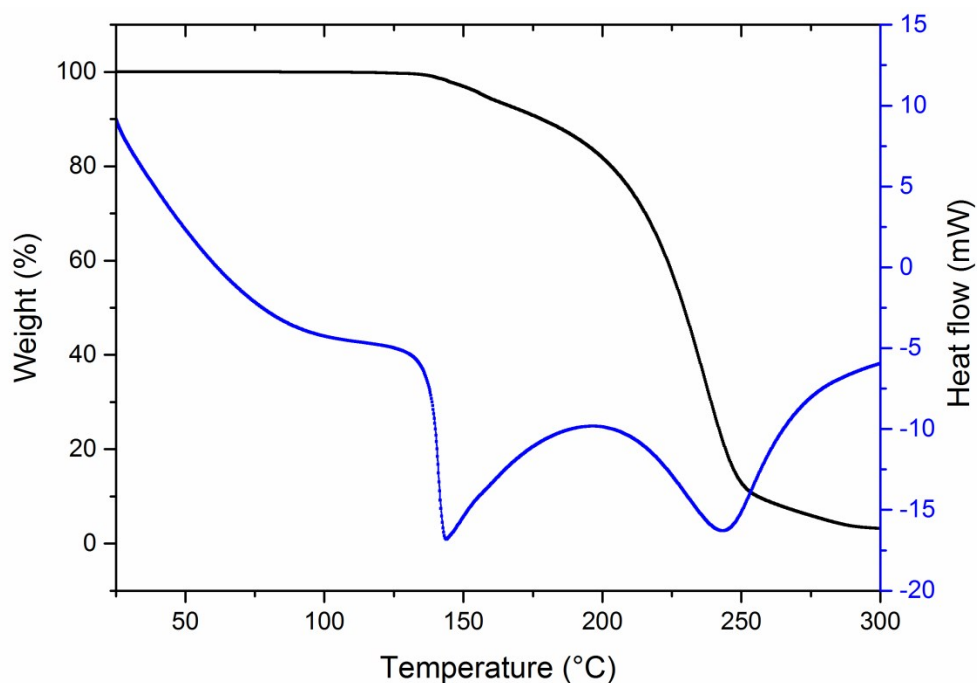


Fig. S9 Thermogravimetry (TG)/differential thermal analysis (DTA) of triflusal-INA cocrystal. Notice that the cocrystal melts at around 135 °C followed by decomposition which is evident by the weight loss and a broad endotherm.

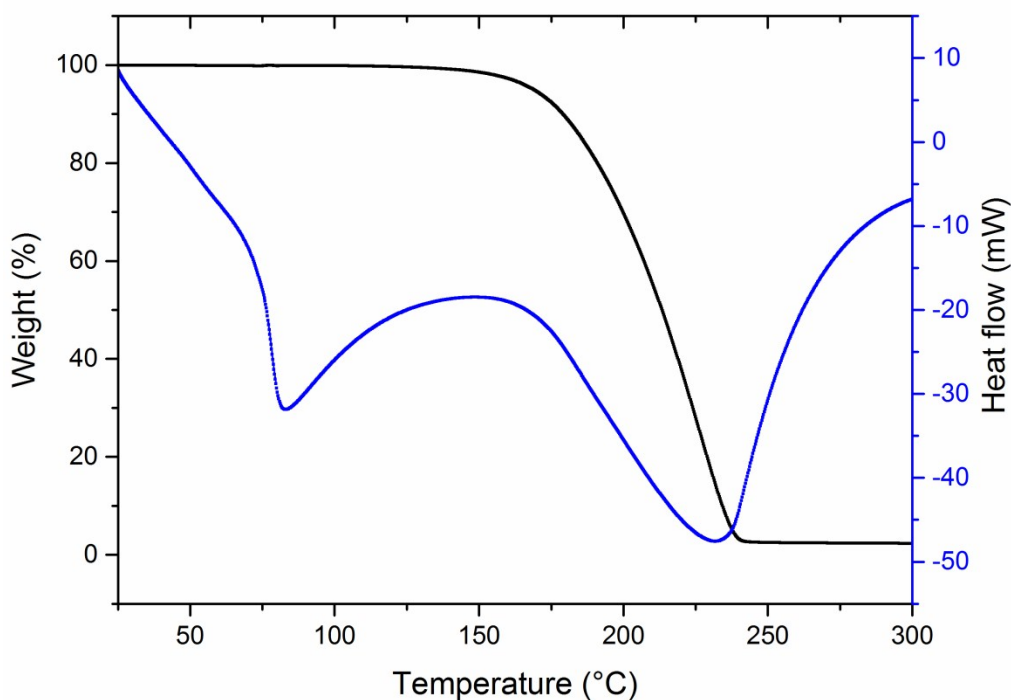


Fig. S10 TG/DTA of triflusal-VA cocrystal. Notice that the cocrystal melts at around 74 °C followed by decomposition which is evident by the weight loss and a broad endotherm.

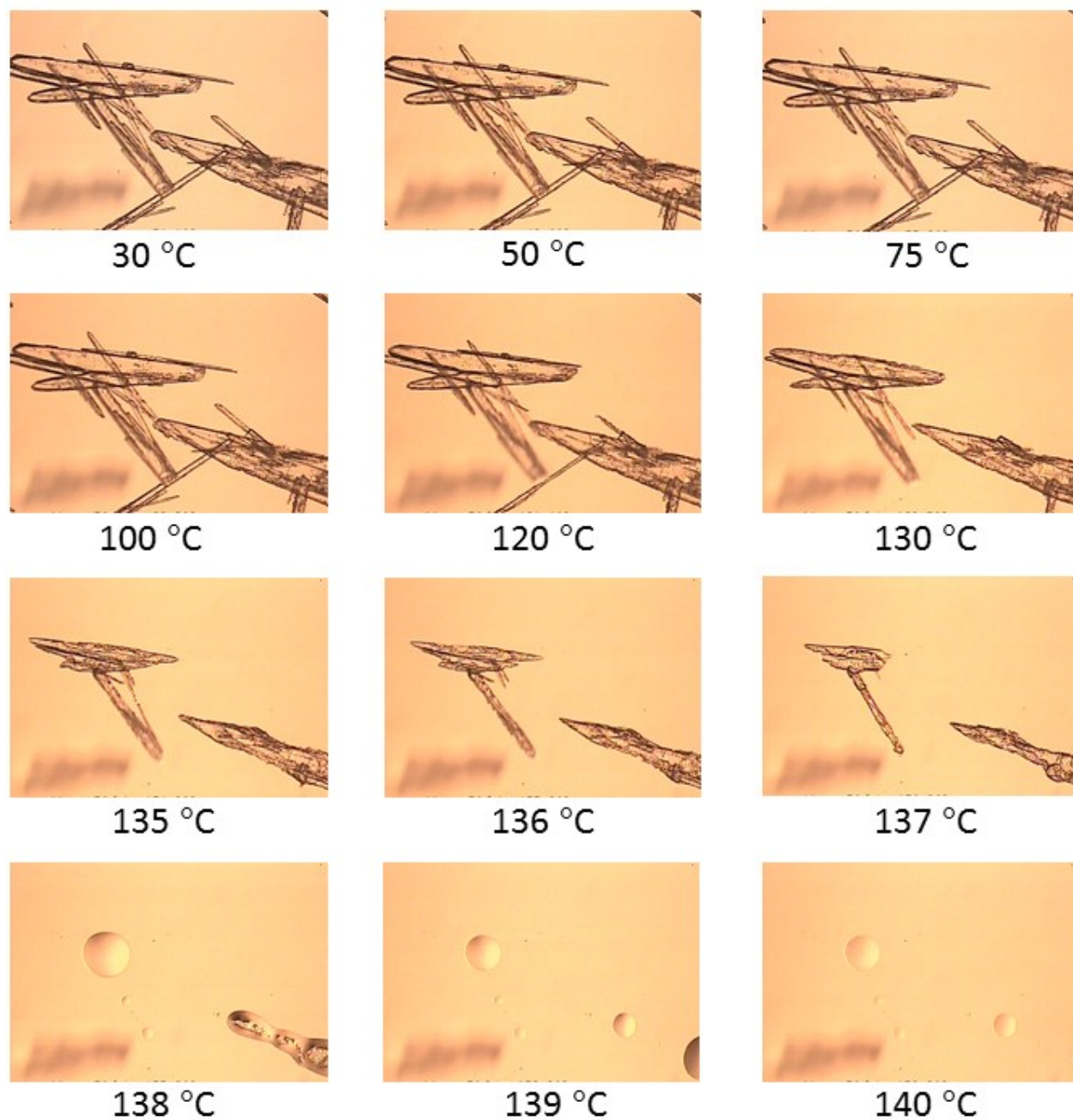


Fig. S11 Photomicrographs of triflusal-INA cocrystal at various temperatures in the HSM experiment. Notice that there was no significant change in the crystals before melting in the temperature range of 135-138 °C.

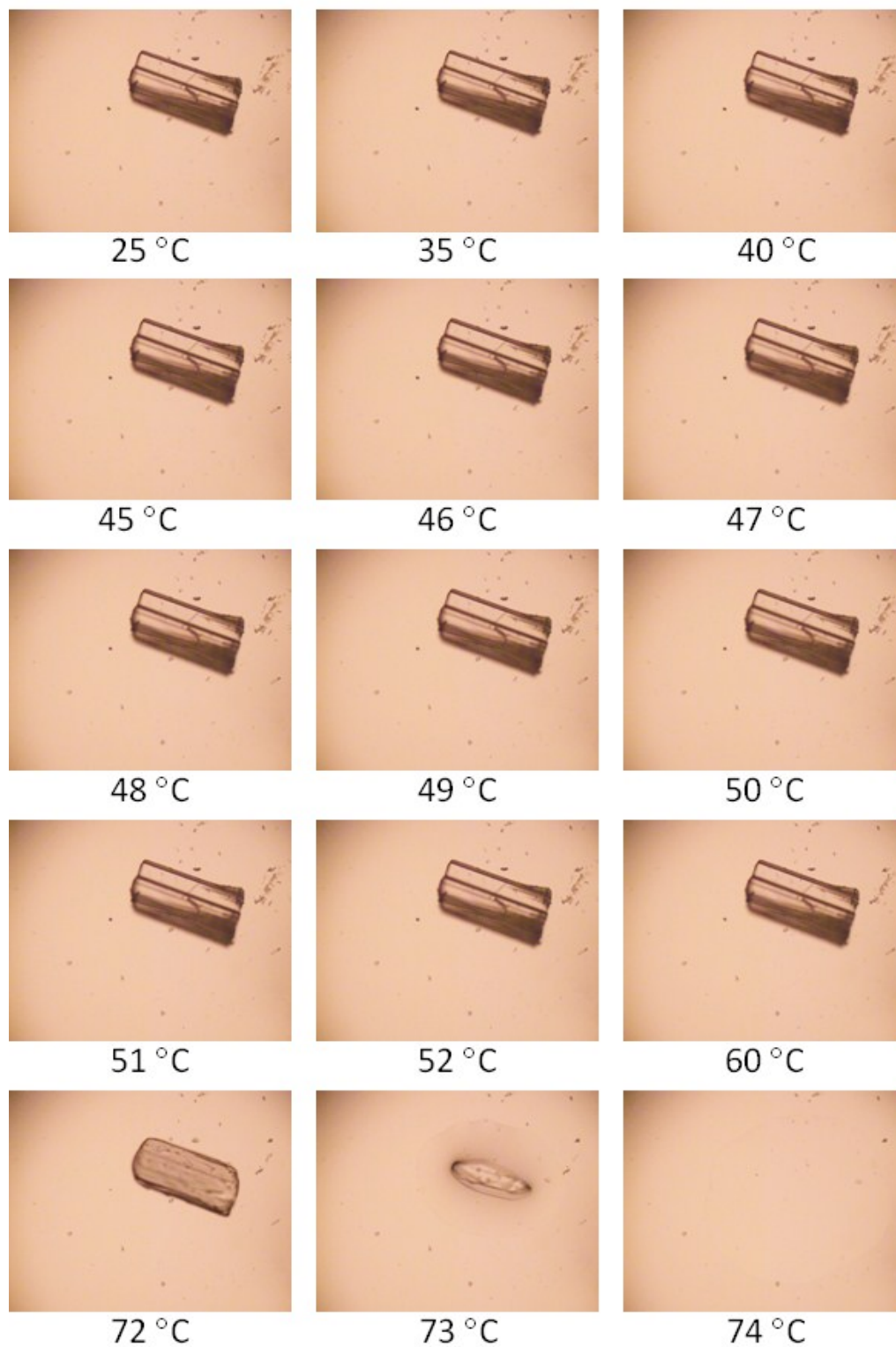


Fig. S12 Photomicrographs of triflusal-VA cocrystal at various temperatures in the HSM experiment. Notice that there was no significant change in the crystal before melting at 73 °C.

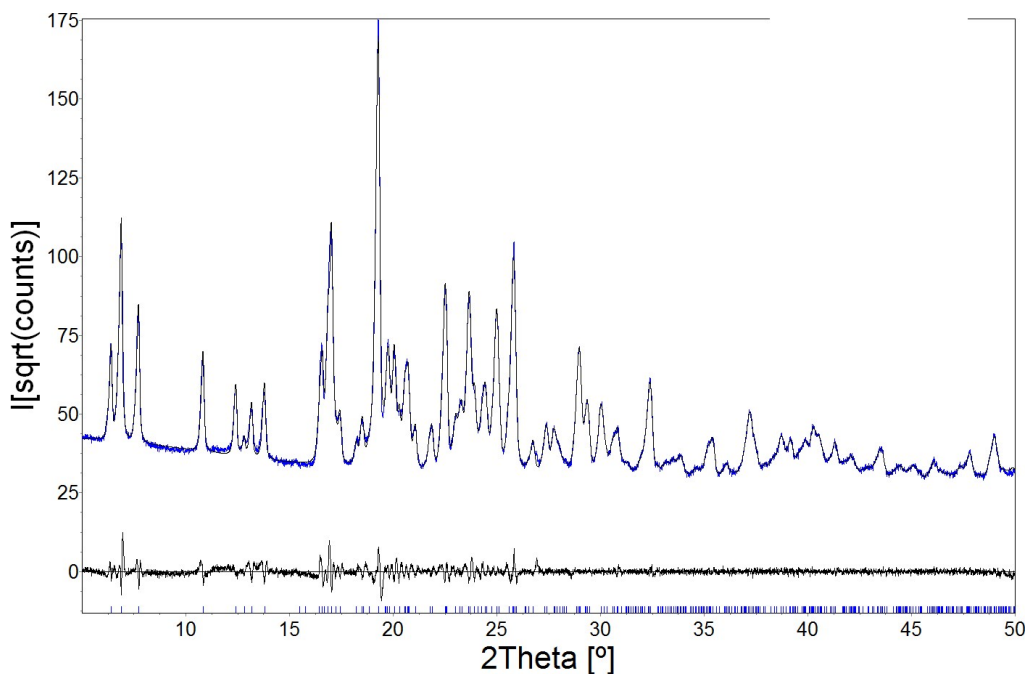


Fig. S13 Pawley fit of room temperature PXRD data of triflusal sample stored at accelerated condition (40 °C, 75 % relative humidity) with unit cell of triflusal from single crystal XRD. The lattice parameters were refined freely.

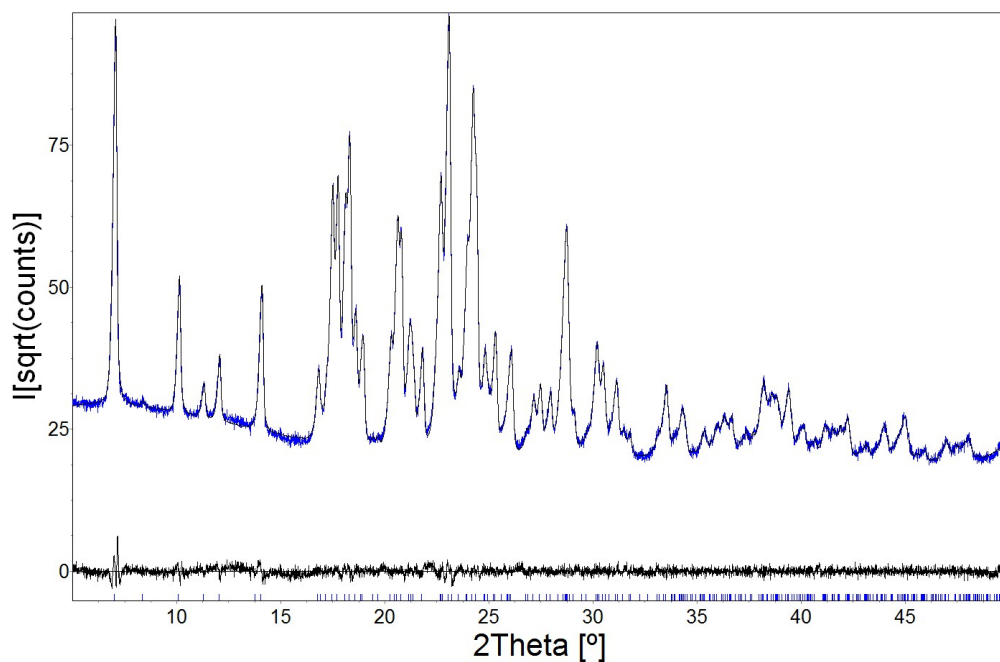


Fig. S14 Pawley fit of room temperature PXRD data of triflusal-BA cocrystal sample stored at accelerated condition with unit cell of triflusal-BA cocrystal from single crystal XRD. The lattice parameters were refined freely.

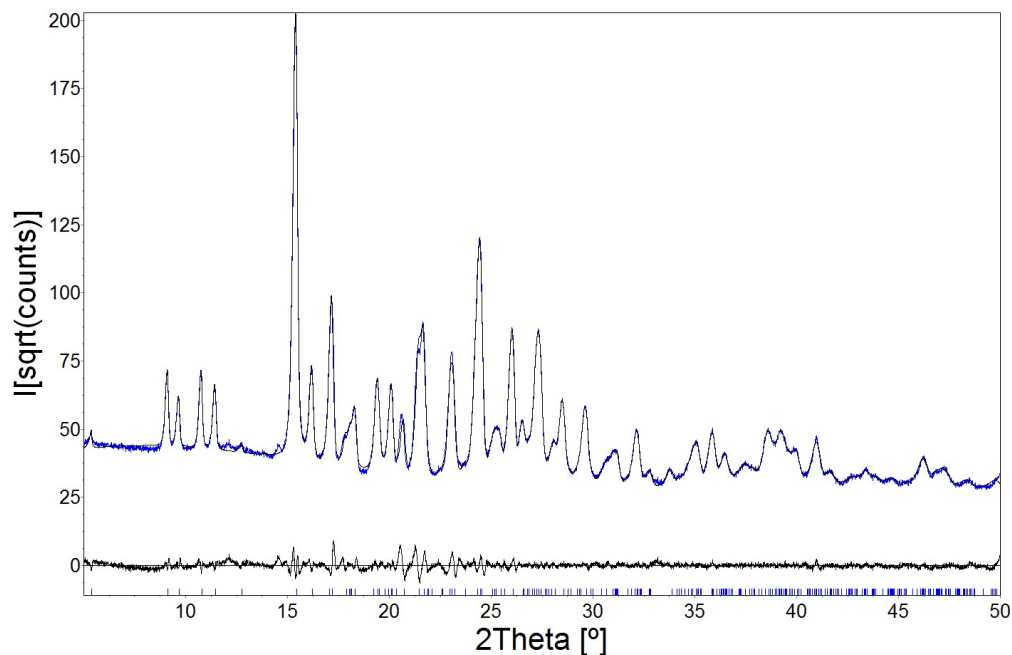


Fig. S15 Pawley fit of room temperature PXRD data of triflusal-INA cocrystal sample stored at accelerated condition with unit cell of triflusal-INA cocrystal from single crystal XRD. The lattice parameters were refined freely.

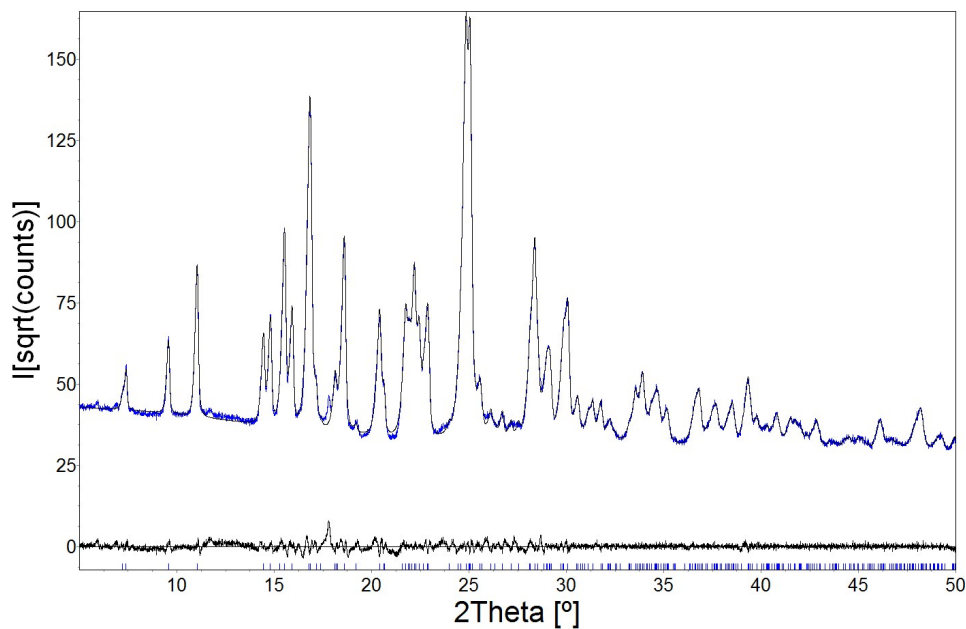


Fig. S16 Pawley fit of room temperature PXRD data of triflusal-PA cocrystal sample stored at accelerated condition with unit cell of triflusal-PA cocrystal from single crystal XRD. The lattice parameters were refined freely.

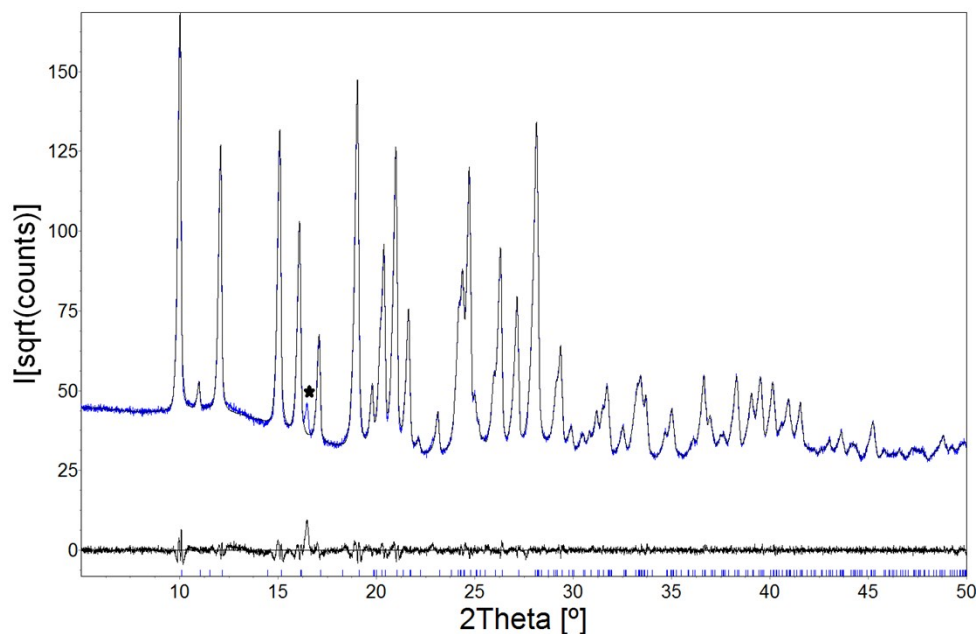


Fig. S17 Pawley fit of room temperature PXRD data of triflusal-urea cocrystal sample stored at accelerated condition with unit cell of triflusal-urea cocrystal from single crystal XRD. The lattice parameters were refined freely. The peak designated with star is unique and do not correspond to any of the starting materials and cocrystal. However, this peak is also present in the powder pattern of the sample obtained from grinding (Fig. S6). Since the powder obtained from grinding experiment was used for stability experiments, the peak is retained.

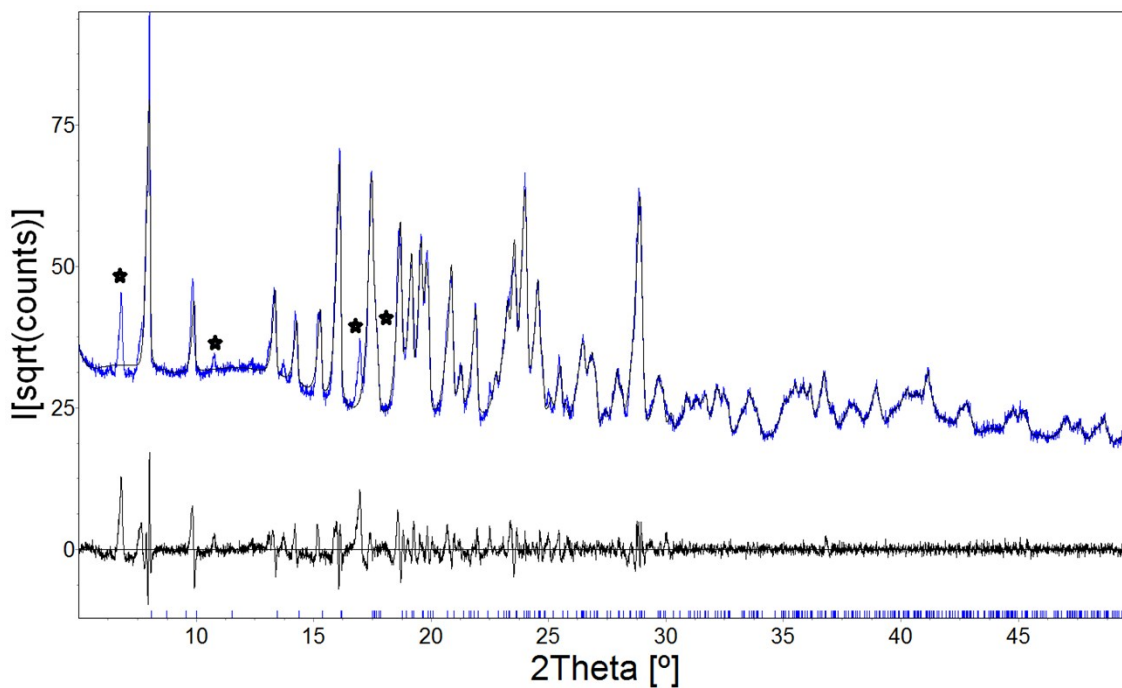


Fig. S18 Pawley fit of room temperature PXRD data of triflusal-VA cocrystal sample stored at accelerated condition with unit cell of triflusal-VA cocrystal from single crystal XRD. The lattice parameters were refined freely. The peaks designated with star correspond to triflusal and VA.

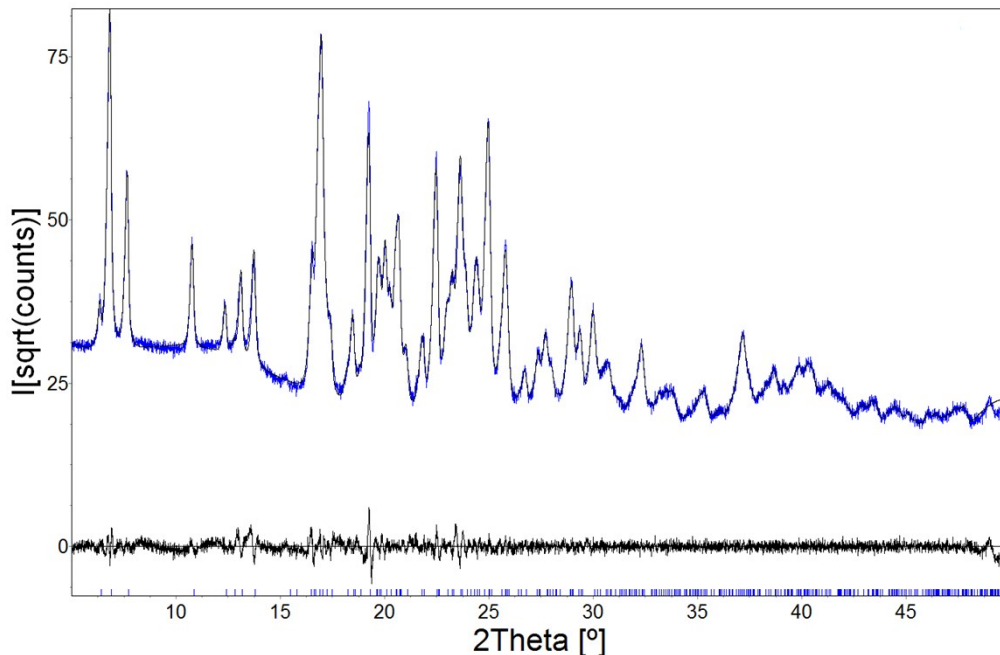


Fig. S19 Pawley fit of room temperature PXRD data of triflusal sample from slurry experiment with unit cell of triflusal from single crystal XRD. The lattice parameters were refined freely.

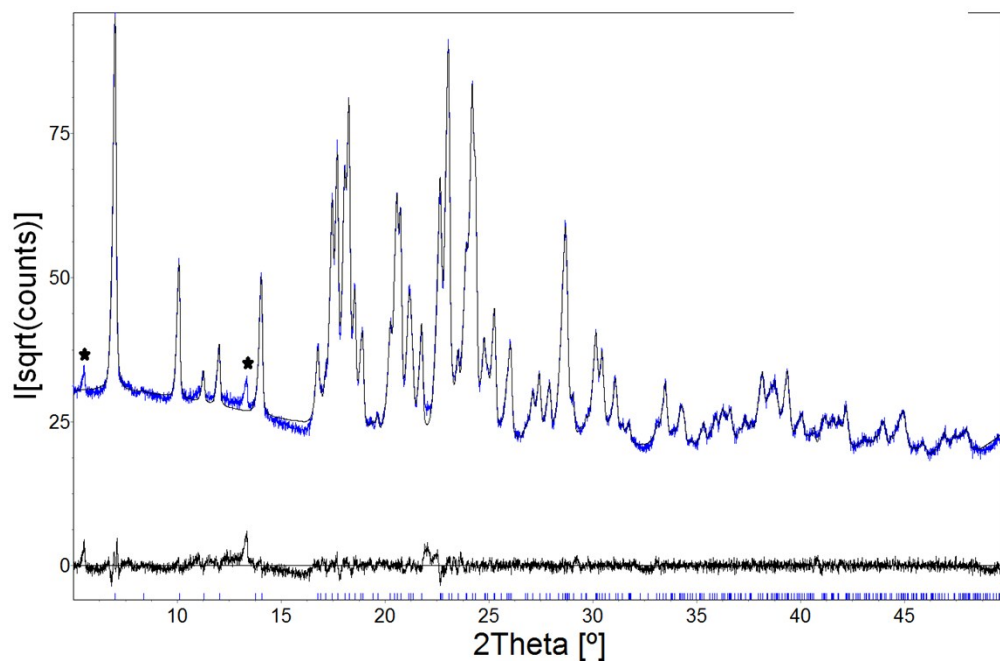


Fig. S20 Pawley fit of room temperature PXRD data of triflusal-BA cocrystal sample from slurry experiment with unit cell of triflusal-BA cocrystal from single crystal XRD. The lattice parameters were refined freely. The peaks designated with star are unique and do not correspond to any of the starting materials and cocrystal. However, these peaks were also present in the powder pattern of the sample obtained from grinding (Fig. S2). Since the powder obtained from grinding experiment was used for stability experiments, the peaks are retained.

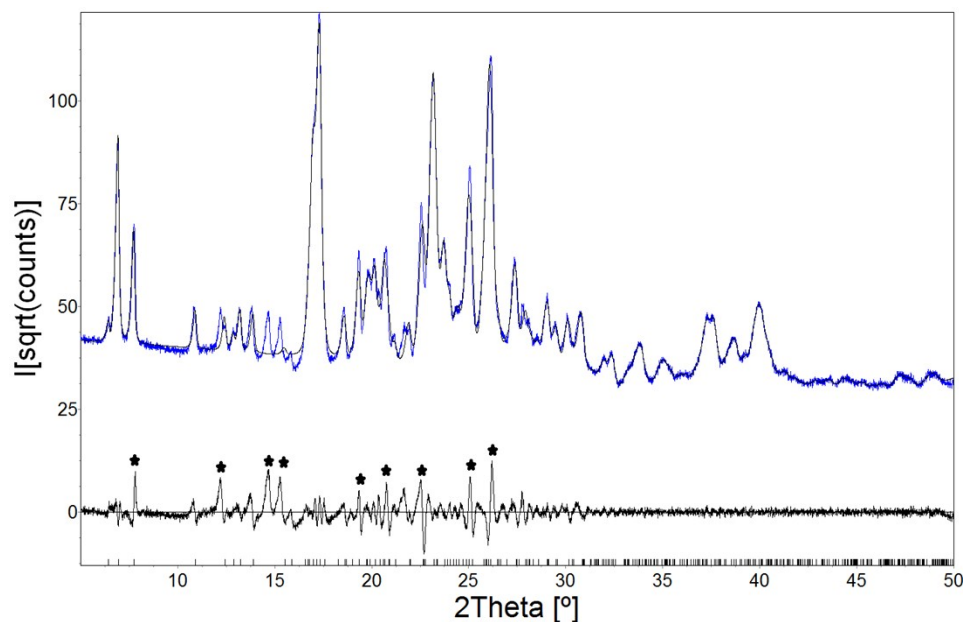


Fig. S21 Pawley fit of room temperature PXRD data of triflusal-INA cocrystal sample from slurry experiment with unit cell of triflusal from single crystal XRD. The lattice parameters were refined freely. The peaks designated with star correspond to HTB.

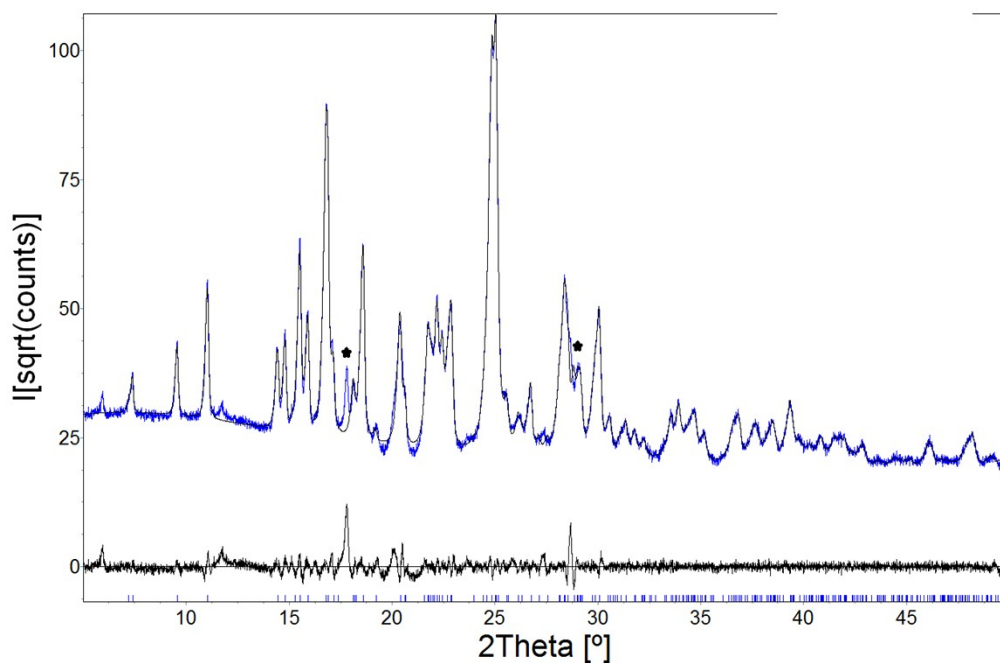


Fig. S22 Pawley fit of room temperature PXRD data of triflusal-PA cocrystal sample from slurry experiment with unit cell of triflusal-PA cocrystal from single crystal XRD. The lattice parameters were refined freely. The peaks designated with star are unique and do not correspond to any of the starting materials and cocrystal.

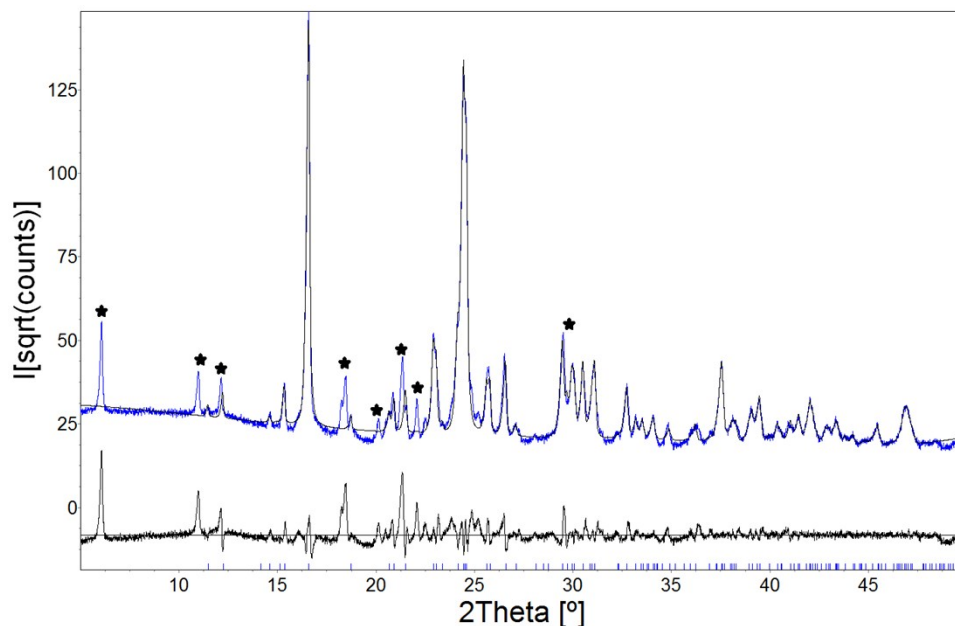


Fig. S23 Pawley fit of room temperature PXRD data of triflusal-PRA cocrystal sample from slurry experiment with unit cell of HTB from single crystal XRD. The lattice parameters were refined freely. The peaks designated with star are unique and correspond to a new phase. Indexing of the new phase provided the unit cell parameters: $a = 29.1238$, $b = 8.3716$, $c = 7.3309$ Å, $\alpha = \beta = \gamma = 90^\circ$, $V = 1787.37$ Å³.

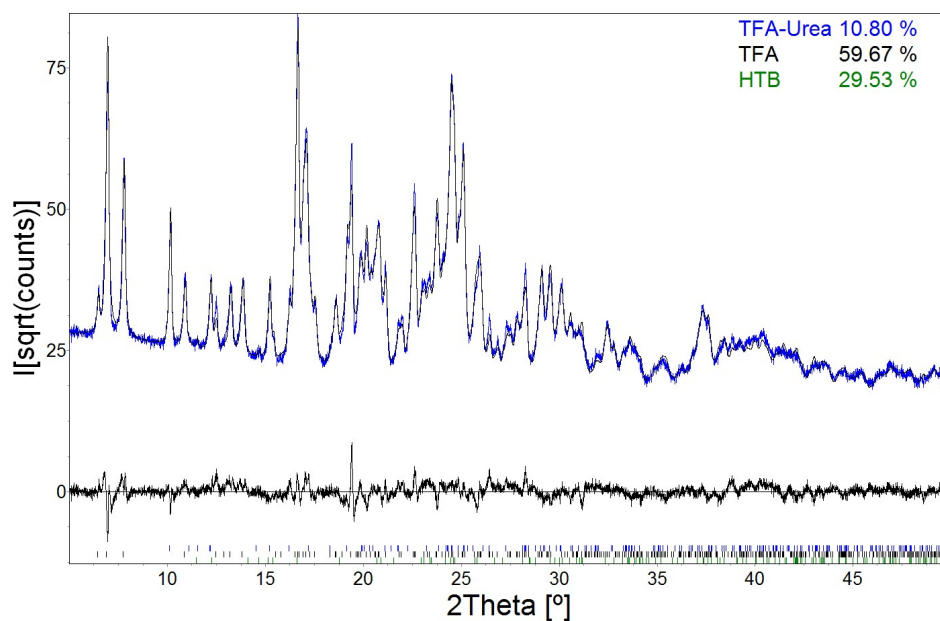


Fig. S24 Rietveld refinement of room temperature PXRD data of triflusal-urea cocrystal sample from slurry experiment with unit cell of triflusal-urea cocrystal, TFA, and HTB from single crystal XRD. The lattice parameters were refined freely. Rietveld refinement of the powder pattern revealed that it contains TFA, HTB, and cocrystal.

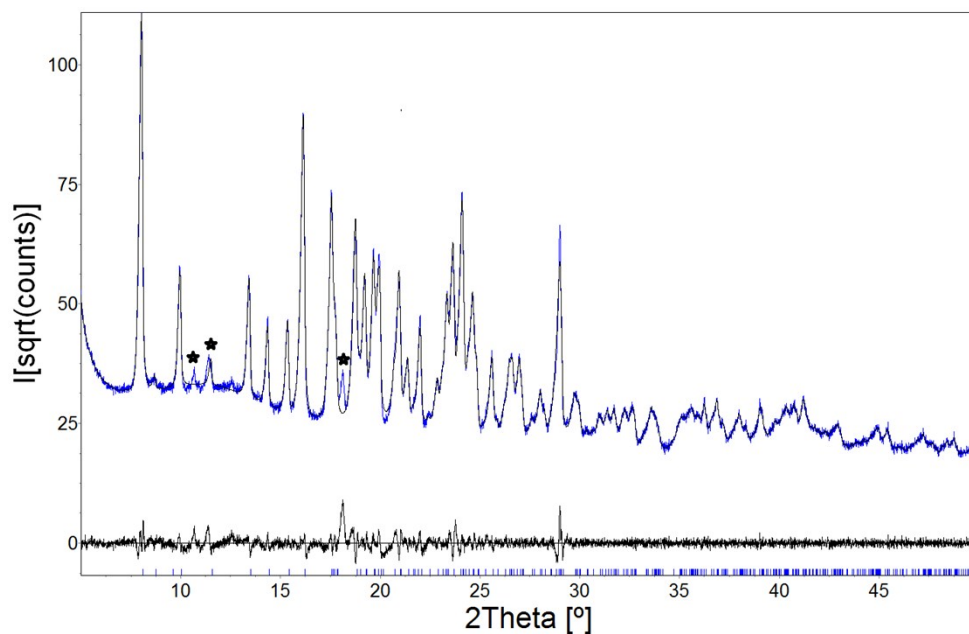


Fig. S25 Pawley fit of room temperature PXRD data of triflusal-VA cocrystal sample from slurry experiment with unit cell of triflusal-VA cocrystal from single crystal XRD. The lattice parameters were refined freely. The peaks designated with star are unique and do not correspond to any of the starting materials and cocrystal. However, these peaks were also present in the powder pattern of the sample obtained from grinding (Fig. S7). Since the powder obtained from grinding experiment was used for stability experiments, the peaks are retained.